

1 Styles of mesoscale brittle deformations associated with the Miocene
2 folding of the Taishu Group, Tsushima, between the Japan Sea and
3 East China Sea backarc basins

4
5
6 Atsushi Yamaji^{1*}, Tatsuhiko Yanagisawa^{1,2}, Katsushi Sato¹

7
8 ¹*Division of Earth and Planetary Sciences, Graduate School of Science, Kyoto*
9 *University, Kyoto 606-8502, Japan*

10 ²*Present address: Itochu Oil Exploration Co Ltd., Kita Aoyama 2-5-1, Minato-ku, Tokyo*
11 *107-0061, Japan*

12
13 *Correspondence

14 E-mail, yamaji@kueps.kyoto-u.ac.jp

15 TEL, 075-753-4266

16
17 Running Title *Folding of the Taishu Group, Tsushima*

20 **Abstract** The Taishu Group is a folded, Eocene–Lower Miocene, thick sedimentary
21 package exposed widely on Tsushima Island between the Japan Sea and East China Sea.
22 This location makes the strata important to understand tectonics and
23 paleo-environments in the Far East, but the timing of the folding is controversial. We
24 studied the styles of brittle deformations of the strata. It was found that flexural-slip
25 folds were dominant. Mesoscale faults were classified into two groups: NE–SW
26 trending reverse faults and NW–SE trending strike-slip faults. Members of both the
27 groups showed movements largely perpendicular to the fold axes. The latter group
28 consisted of sinistral and dextral faults. Accordingly, we interpreted that they were
29 transfer faults activated during the folding. Consequently, mesoscale faults and
30 flexural-slip faults evidence the map-scale plane strain of the Taishu Group in the plane
31 perpendicular to the NE-trending fold axes. There were few transpressional
32 deformations in the group. This is inconsistent with the transpression hypothesis for
33 explaining the simultaneous folding and Japan Sea opening. Another hypothesis in
34 which the folds in Tsushima are regarded as an onshore part of the Taiwan-Shinji fold
35 belt is inconsistent with the timing of folding suggested by mining geologists to be
36 consistent with and contemporaneous with this deformation. On the other hand, we
37 found that dolerite dikes and sills were involved in the folding. Therefore, we conclude
38 that the folding began during the late Early Miocene time and climaxed during the ore
39 mineralization at around 15 Ma. We suggest that the folding in Tsushima was the
40 easternmost manifestation of the compressional regime around the Yellow Sea and East
41 China Sea in the Early to early Middle Miocene, and that the compression was brought
42 about by the arrival of the Philippine Sea plate to initiate buoyant subduction under
43 Kyushu.

44

45 **Key words:** flexural-slip fold, bedding-parallel fault, transfer fault, Taiwan-Shinji fold
46 belt, Japan Sea opening

47

48

49 **1 INTRODUCTION**

50

51 The geology of Tsushima Island is a key to understand tectonic and climatic evolution
52 of the Far East, because it is a large island rising in the straight between the Japan Sea
53 and East China Sea backarc basins behind the Japan and Ryukyu island arcs (Fig. 1a).
54 Folded Cenozoic strata, called the Taishu Group, are widely exposed in Tsushima (Fig.
55 1b). The folding may have led to the uplift of the straight that could affect the

56 environments of the Far East (e.g., Chinzei, 1986; Kimura et al., 2004; Kitamura &
57 Kimoto, 2006; Millien-Parra & Jaeger, 1999). However, the timing of folding is
58 controversial.

59 Two hypotheses have been proposed for the timing. The first one attributes the
60 folding to the inferred transpression at the southwestern end of the rapidly opening
61 Japan Sea in the early Middle Miocene (Fabbri et al., 1996; Golozubov et al., 2017;
62 Ishikawa & Tagami, 1991; Kim et al., 2008, 2010; Sakai, 1993). This hypothesis is
63 consistent with the presence of the offshore Tsushima Fault System (Fig. 1a) along the
64 western coast of Tsushima (Tomita et al., 1975), which was possibly a major dextral
65 strike-slip fault during the Japan Sea opening (e.g., Jolivet et al., 1991). Folds in the
66 island make, indeed, an echelon pattern with respect to the fault (Fig. 2a). The second
67 hypothesis regards the folds as the onshore parts of the Taiwan-Shinji fold belt (Fig. 1a),
68 which was formed mainly in the Late Miocene (Cukur et al., 2011; Gungor et al., 2012;
69 Kong et al., 2000; Lee et al., 2006, 2011; Tai, 1973; Tanaka & Ogusa, 1981; Yoshioka et
70 al., 2002).

71 However, the geologists of Taishu Mine in southern Tsushima (Fig. 1b) expressed
72 another view based on their observations in the mine, where mesothermal veins were
73 worked (e.g., Kiyosu, 1977; Shimada, 1977). Ikemi et al. (2001) obtained a K-Ar age of
74 15.4 ± 0.8 Ma (Ikemi et al., 2001) from an ore vein. Older ore veins were deposited on
75 thrust faults with NW-vergence (Matsuhashi, 1967, 1968), and late Early to early
76 Middle Miocene felsic sills were involved in the thrusting (Uehara, 1959; Uehara &
77 Matsuhashi, 1961; Shimada, 1977). They considered that the Taishu Group was folded
78 shortly before or simultaneously with the formations of older veins (e.g., Shimada,
79 1977). This seems consistent with the first hypothesis, above, in the timing of folding,
80 but with the second one in the vergence. Unfortunately, the mine has been abandoned
81 since 1973, so the validity of their opinion is uncertain.

82 The purpose of this paper is to describe mesoscale deformation structures observed
83 at outcrops in the Taishu Group to verify the three hypotheses including the opinion of
84 the mining geologists. That is, transpression of the first hypothesis should involve either
85 (1) flexural-slip faulting oblique to the NE-trending fold axes (Tanner, 1998, Fig. 19) or
86 (2) the intermingled distribution of folds, thrusts and strike-slip faults with similar
87 trends (Figs. 2a, b) (e.g., Holdsworth et al., 2002; Jones et al., 2004; Tavarnelli et al.,
88 2004) or (3) both. On the other hand, the second hypothesis expects the shortening of
89 the crust that could be accommodated by flexural-slip faulting perpendicular to the fold
90 axes and by reverse faulting with NW or NE vergence. We also investigated the relative
91 timing of igneous intrusion and the deformations accompanied by the folding. However,

92 it is beyond the scope of this paper to argue fully about the basin formation of the
93 Taishu Group and about the opening or closure of backarc basins. We describe
94 mesoscale tectonic deformations to test the three hypotheses.

95

96 **2 GEOLOGICAL BACKGROUND**

97

98 The Taishu Group is thought to be Eocene–Early Miocene in age. Deltaic to submarine
99 slope or to basin settings are inferred for the depositional environments of the strata
100 (Koga et al., 1988; Nakajo et al., 2006; Nakajo & Maejima, 1998; Ninomiya et al., 2009,
101 2010, 2020; Okada & Fujiyama, 1970). The folded Taishu Group is unconformably
102 covered by Upper Pliocene sediments (Isomi & Nagahama, 1965). The group is
103 composed of three informal units—the Lower, Middle and Upper Formations
104 (Matsumoto, 1969) (Fig. 1b). The Lower and Upper Formations are composed of
105 alternating sandstone and shale; the Middle Formation consists of massive mudstone
106 and shale. Mudstones have locally incipient slaty cleavage (Fig. 3) (Oho *et al.*, 2007).
107 The total thickness of the group is thought to be greater than 4 km, but is uncertain
108 because of its controversial stratigraphy.

109 The stratigraphy of the group is a matter of debate (Miyata, 2010) owing to
110 monotonous lithology, complicated structures and sparse inland outcrops. The Taishu
111 Group has so complicated map- and mesoscale structures that bedding attitudes at
112 neighboring outcrops are often discordant with each other and with uncertain
113 stratigraphic relations. So, we did not draw geological maps, but dealt with mesoscale
114 structures.

115 Radiolarian fossils indicate that the Lower Formation is Early Eocene in age
116 (Nakajo & Funakawa, 1996). Pyroclastic rocks in the Middle Formation yielded the
117 fission track ages of the mid Eocene (Sakai & Yuasa, 1998). Lower part of the Upper
118 Formation yielded Early Miocene planktonic foraminifers (Ibaraki, 1994), but a middle
119 horizon of the formation yielded Oligocene ones (Sakai & Nishi, 1990). In addition,
120 Ninomiya et al. (2014) reported the U-Pb ages of ~18 and ~16 Ma from the tuffs that
121 defined the boundary between the Lower and Middle Formations.

122 The Taishu Group is intruded by plagiophyre, quartz porphyry and granite with a
123 minor amount of dolerite sheets and dikes. The granite was crystallized at a depth of
124 2–6 km (Shin et al., 2009). All those rocks yielded K-Ar and fission-track ages between
125 12 and 19 Ma (Ishikawa & Tagami, 1991; Karakida, 1987; Takahashi & Hayashi, 1985,
126 1987). Detailed geochemical study by Ikemi et al. (2001) showed with K-Ar
127 thermochronology that the granite cooled down from 560 to 350°C in the period from

128 17 to 14 Ma and formed Pb-Zn deposits of the Taishu mine at ~15 Ma. Though various
129 ages from 17 to 12 Ma were reported from the granite (Ikemi et al., 2001; Ishikawa &
130 Tagami, 1991; Karakida, 1987; Kono & Ueda, 1966), the granite was emplaced
131 probably at 17–18 Ma. Muscovite in an ore vein yielded a K-Ar age of 15.4 ± 0.8 Ma
132 (Ikemi et al., 2001). The dolerite is thought to be as old as the felsic magmatism
133 (Matsumoto & Takahashi, 1987). Felsic and mafic magmatism in Miocene Tsushima
134 resulted probably from the same mantle upwelling event (Shin et al., 2009).

135 Offshore seismic survey near Tsushima showed that the Tsushima fault system was
136 activated as a thrust system sometime in the Late Miocene or Pliocene (Minami, 1979),
137 thereby the islands were uplifted. A seismic profile along a transect across the
138 Taiwan-Shinji fold belt some 20 km to the northeast of Tsushima (Itoh & Nagasaki,
139 1996) visualized an anticlinorium involving Miocene and older rocks on the
140 northeastern extension of the fold axes from Tsushima Islands, and showed the thinning
141 of Pliocene-Quaternary offshore sediments toward the anticlinorium. The profile
142 suggests an uplift of Tsushima by a few hundred meters after the Miocene. Marine
143 terraces on Tsushima Islands evidence a slow uplift in the mid Pleistocene at a rate of
144 10^1 m/m.y. (Watanabe & Ikeda 1989). Offshore seismic profiles suggest that the
145 Tsushima fault system is inactive (e.g., Tokuyama et al., 2001).

146

147 **3 MESOSCALE DEFORMATION STRUCTURES**

148

149 **3.1 Fold geometry**

150 There are map-scale and mesoscale folds in the Taishu Group, but thick vegetation
151 hinders most of the hinge zones. Accordingly, we investigated the shapes and
152 orientations of map-scale folds from bedding attitudes of neighboring fold limbs (Fig. 4).
153 Slump folds are not rare in the group (Golozubov et al., 2017; Nakajo et al., 2006), but
154 folds with tectonic origin were more abundant than slump folds. The tectonic origin was
155 evidenced by the involvement of brittle deformations (Fig. 5). In each area in Tsushima,
156 the orientations of fold axes were calculated from the orientation matrix of the poles to
157 bedding (e.g., Scheidegger, 1965). That is, given bedding attitudes in neighboring limbs,
158 the eigenvector corresponding to the minimum eigenvalue of the matrix was regarded as
159 the fold axis. The intersections of the great-circles that indicate bedding attitudes made a
160 small cluster around the eigenvector (Figs. 4a–k), meaning that the folds in the areas
161 were cylindrical. In addition, the bedding attitudes had more or less two clusters in the
162 stereograms, representing the planar limbs of chevron folds (Twiss & Moores, 2006).
163 They had interlimb angles ranging from 50 to 150°, but isoclinal folds were found to the

164 west of the Taishu mine. The orientations of axial planes were estimated to be roughly
165 vertical from the bisector of the limb orientations.

166 The Osaki area (Fig. 1b) is one of the areas in Tsushima where short-wavelength
167 folds were found, allowing us to recognize fold styles easily. Therefore, we made field
168 survey mainly in the area. The Lower Formation in this area is composed of shale,
169 massive mudstone and mudstone-dominant alternation of sandstone and mudstone.
170 Complicated geologic structures impeded geological mapping. So, we present a
171 geological route map of this area (Fig. 6). We recognized tens of fold hinge lines in the
172 Osaki area with the wavelengths of 10^1 – 10^2 meters. Fig. 6a shows the orientations of 31
173 hinge lines of folds, indicating their mean orientation around $050^\circ/20^\circ$. Bedding
174 attitudes in neighboring limbs indicated that the folds were cylindrical in shape. This is
175 evidenced by the great circles representing the bedding that intersect each other around
176 a point in each of the stereograms in Fig. 4.

177 Folds had typical wavelengths of ~ 150 m along the northern coast of the Osaki area
178 (Fig. 6b), but those folds did not extend southwestward along their trend into the
179 western coast of the area around Cape Kottoi. There was no such short-wavelength fold
180 there. This discontinuity suggests the presence of one or more map-scale transfer faults,
181 low-angle faults or an angular unconformity between Kottoi and the northern coast, but
182 thick vegetation hindered the boundary(s) and made geological mapping unattainable.

183 3.2 Bedding parallel faults

184 All the folds that we observed in the Taishu Group involved bedding-parallel faults
185 (Figs. 7, 8). They were recognized by the offset or truncation of veins, faults, sole marks,
186 etc., along bedding (Cloos, 1948; Fitches et al., 1986). Bedding planes with slickenside
187 striations or slickenfibers were recognized as bedding-parallel faults as well. The sense
188 of faulting was determined by a few criteria, i.e., the offset of those features intersecting
189 the fault plane, the accretion steps of the fibers, the asymmetric striations made by
190 ploughing particles (Petit, 1987).

191 Folds in the Taishu Group were formed by flexural-slip mechanism (Kim et al.,
192 2008). There are two lines of evidence. First, the slip directions of bedding-parallel
193 faults were roughly perpendicular to the fold axis that was determined by the bedding
194 attitudes in neighboring fold limbs (Figs. 6, 8). Second, most of the faults upon which
195 the sense was determined were reverse in sense, though the sense of movement was
196 determined only on a small number of bedding-parallel faults. There were a few
197 exceptions, which were nearly upright normal faults at Shiine (Fig. 4j). Since those
198 faults were found in overturned strata, they may have been originally reverse faults
199 overturned by folding. Arrows and bars on the stereogram in Fig. 8 show the slip

200 directions and orientations, respectively, of bedding-parallel faults. Most of the symbols
201 are drawn along the great- and small-circles with the pole that is parallel to the mean
202 orientation of the fold axes. Therefore, bedding-parallel faults indicate nearly plane
203 strain in the plane perpendicular to the mean orientation.

204 We found that ore veins near Taishu Mine were affected by the flexural-slip folding.
205 That is, bedding surfaces coated by the quartz veins that bore sphalerite, pyrrhotite and
206 magnetite (Fig. 9) had slickenside striations perpendicular to the general trend of the
207 fold axes (Fig. 4). The ore veins of the mine were characterized by those minerals
208 (Uehara, 1959).

209 3.3 Mesoscale faults cutting across bedding

210 We collected fault-slip data not only from bedding-parallel faults but also from
211 mesoscale faults across strata. They had thin shear zones less than 1 cm in thickness.
212 The sense of faulting was determined by the offsets of strata or by the asymmetrical
213 minor structures on the fault surfaces, which were mentioned in the last subsection. To
214 investigate syn-sedimentary tectonics Fabbri et al. (1996) and Kim et al. (2010)
215 described such faults that were accompanied by soft-sediment deformations. However,
216 we dealt only with brittle faults, because evidence for faulting involved in such
217 deformations were rare, and because this paper aims at describing post-depositional
218 deformations.

219 Figure 10 shows fault-slip data mainly from the Osaki area. The orientations of
220 fault planes had a large variation, but their poles made two clusters. The mean
221 orientation of fold axes is plotted in the figure as well. The most prominent cluster was
222 made from NW–SE trending, nearly upright, strike-slip faults: Sinistral and dextral
223 strike-slip faults were mixed in this group. Both the slip directions and fault planes were
224 approximately perpendicular to the mean of the fold axes. That is, their tectonic
225 transport directions were roughly the same with the trends of horizontal shortening by
226 the flexural-slip folding. We interpreted that the faults were the transfer faults (e.g.,
227 McClay, 1992, p. 430) accompanied by the folding. This is supported by simultaneous
228 activity of such strike-slip faults and bedding-parallel faults, evidenced by their
229 crosscutting relationships (Fig. 11). Florez-Nino et al., (2005) reported pervasive, minor
230 transfer faults in a fold and thrust belt in Bolivia.

231 The second prominent cluster appeared in the NW quadrant in the tangent-lineation
232 diagram in Fig. 10. Most of the faults corresponding to this cluster were SE-dipping
233 reverse faults. There were many faults with the symbols out of the two clusters. It
234 should be noted that most of the arrows and bars corresponding to those faults are
235 parallel to the great- and small-circles with the pole parallel to the mean fold axis.

236 In conclusion, most of the mesoscale faults plotted in Fig. 10 had tectonic
237 transports more or less perpendicular to the mean orientation of the fold axes.

238 3.4 Dolerite sheets and dikes

239 In this study, doleritic sills and dikes in the Taishu Group were found to be affected
240 by the folding. For example, the dolerite sheets shown in Fig. 12a were folded with the
241 host strata. The hinterland-dipping duplex shown in Fig. 12b involved a dolerite sheet,
242 the fault slices of which were bounded by thrust faults with tectonic transport directions
243 roughly perpendicular to the general trend of folds (Fig. 12a). Accordingly, the fault-slip
244 data from the duplex suggested the simultaneous formation of the duplex with the
245 folding.

246 Dolerite dikes were also affected by the folding as well. Figure 13a shows a dolerite
247 dike involved in a duplex with a NE–SW trending flexural-slip fault with NW–SE striae.
248 Figure 13b shows an NW–SE trending dolerite dike involved in a strike-slip duplex.
249 This deformation is consistent with the horizontal shortening in this trend by folding.
250 This interpretation is supported by the fault-slip analysis of the faults involved in this
251 duplex: We obtained NW–SE compressional stress from them (Fig. 14b) using the
252 method of Sato (2006).

253

254 4 DISCUSSION

255 4.1 Deformation of the Taishu Group

256 The flexural-slips perpendicular to the general trend of fold axes were pervasive in the
257 Taishu Group (Figs. 4, 8). The flexural slip folding resulted in the macroscale plane
258 strain of the strata in the vertical plane parallel to the NW–SE trending tectonic
259 transport by the flexural folding. The fold in the Unatsura area was an exception: The
260 fold had bedding-parallel faults with striae not perpendicular to the fold axis (Fig. 4f).
261 The striae leaning toward the southwestward plunging fold axis can be ascribed not to
262 transpressional tectonics but to a tilting of strata before folding (Ramsay, 1967) or to a
263 locally developed three-dimensional, flexural-slip folding (Tanner, 1989). Most of the
264 tectonic transports by brittle faulting in the strata had roughly the same trend (Fig. 10).
265 Both the reverse faults and NW–SE trending transfer faults among them are consistent
266 with the plane strain in a map-scale. This is consistent also with the fact that a NW–SE
267 trending joint system is dominant in the Taishu Group (Kitamura, 1962).

268 The folds in Tsushima have often been regarded as the en echelon folds (e.g., Silver,
269 1988) formed by the left-lateral movement of the Tsushima fault system (Figs. 1, 2)
270 (Fabbri et al., 1996; Inoue, 1982; Ishikawa & Tagami, 1991; Kim et al., 2010). We are
271 opposed to this hypothesis. The strike-slip faulting that forms such drag folds has

272 various subsidiary faults oblique to the master fault. The trends of such faults have
273 systematic relationship with the senses of faulting such as R and R' shears (e.g., Silver,
274 1988). However, there was no such systematic relationship in the mesoscale faults that
275 we observed in Tsushima (Fig. 10). Wilcox et al. (1973) found in their clay models that
276 inter-layer sliding was needed to form en echelon folds in wrench tectonics. Slip vectors
277 on bedding-parallel faults in a transpressional deformation zone are systematically
278 rotated clockwise or counterclockwise (Holdsworth et al., 2002; Tanner, 1989), resulting
279 in a triclinic strain of the zone (Tavarnelli et al., 2004). However, the orthogonality
280 between fold axes and flexural-slip directions implies the absence or negligible amount
281 of strike-slip component in the bulk strain of the Taishu Group during folding.

282 To investigate regional tectonics, previous researchers inverted fault-slip data
283 obtained from mesoscale faults in the Taishu Group (Fabbri et al., 1996; Kim et al.,
284 2008, 2010), but we did not. The reason why we did not study paleostresses was the
285 difficulty to retrorotate fault-slip data to compensate tilting and paleomagnetic rotation.
286 That is, the strata of the group had usually the dip angles of 30° or more. (The data set
287 in Fig. 14b is an exception, because all the data were obtained around a dike where the
288 host strata were approximately horizontal.) In addition, the strata were subjected to
289 counterclockwise paleomagnetic rotations by 20–30° (Ishikawa et al., 1989). Kim and
290 others report extensional stress during the accumulation of the Taishu Group from such
291 mesoscale faults that were accompanied by soft-sediment deformations (Kim et al.,
292 2008, 2010). They applied horizontal- and vertical-axis rotations to their fault-slip data
293 for restoring fault attitudes. However, such finite rotations are affected by the order of
294 rotations. The relative timing of the rotations is not clear. Fabbri et al. (1996) did not
295 refer to the tilt correction of the fault-slip data. To investigate paleostress further from
296 faults in the strata, stress tensor inversion combined with tilt correction (e.g., Tonai et al.,
297 2011; Yamaji et al., 2005) must be applied to faults in the strata. Shimada (1977) and
298 Golozubov et al. (2017) showed the dominant NW-SE trend of mineral veins in areas
299 far from Taishu Mine. The veins indicate the σ_{Hmax} -axis perpendicular to the general
300 trend of folds: Folding could have hardly influenced the dominant trend if the veining
301 predated the folding. However, the formation age(s) of the veins are unknown.

302 4.2 Timing of folding

303 The timing of folding of the Taishu Group is controversial. Offshore seismic surveys
304 indicate the formation of the Taiwan-Shinji fold belt mainly in the Late Miocene, but it
305 is not obvious whether the folds in the group are the onshore parts of the fold belt or
306 older structures. Matsumoto and Takahashi (1987) investigated the modes of occurrence
307 of intrusive rocks in Tsushima, thereby argued the timing of folding. They found that

308 constant thickness of plagiophyre sills in neighboring limbs of folds, and concluded that
309 the intrusion predated the folding. Plagiophyre in Tsushima gave a fission-track age of
310 18–19 Ma (Takahashi & Hayashi, 1985). In addition, we found in this study that
311 dolerites were involved in the folding. The mafic magmas under Tsushima were
312 generated simultaneously with felsic ones including granitic magma in southern
313 Tsushima by the same mantle upwelling event (Shin et al., 2009). Those observations
314 suggest that all or most of the magmatism in Tsushima predated the folding. Okada
315 (1969) reported a doleritic phacolith with a lateral dimension of ~1 km in northern
316 Tsushima, thereby he suggested the intrusion being simultaneous with folding. However,
317 thick vegetation makes it difficult to see whether the lateral variation in thickness of a
318 map-scale intrusive body was affected by folding. Thick vegetation may hide a thrust
319 duplex that apparently doubled a sill thickness.

320 Mining geologists considered that the veining in Taishu Mine was
321 contemporaneous with and shortly after the folding (Matsushashi, 1967, 1968; Uehara,
322 1959; Uehara & Matsushashi, 1961). The ore veins were formed in the late cooling stage
323 of the granitic pluton emplaced in the southern part of Tsushima: Muscovite from an ore
324 vein gave the K-Ar age at 15.4 ± 0.8 Ma (Ikemi et al., 2001). The geologists of the mine
325 classified ore veins into older ‘bedding’ and younger ‘N-S trending’ groups, which were
326 formed on southeastward dipping faults. Matsushashi (1967, Fig. 9; 1968, Fig. 7)
327 described the precipitation of ore veins preferentially at dilational jogs in duplexes upon
328 bedding-parallel faults, though he used the term ‘drag folds’ upon bedding-parallel
329 faults instead of ‘duplexes.’ The latter term has become popular after Elliott and
330 Johnson (1980) and Suppe (1983). Matsushashi revealed the NW vergence of the
331 deformation as well. The ‘bedding’ group was also formed as saddle and trough reefs
332 (Fig. 15). Quartz porphyry sills were observed in the mine to be affected by the thrust
333 faults that hosted the ‘bedding’ veins. Quartz porphyry intruded the Taishu Group in late
334 Early to early Middle Miocene (Fig. 16). Those descriptions are consistent with the
335 deformations that we observed at outcrops (Section 3). The observations of the ‘bedding
336 group’ evidence the simultaneity of their deposition and folding, but do not disprove the
337 beginning of the folding prior to the veining.

338 Although earlier studies suggested that the ‘N-S trending group’ were formed along
339 easterly dipping normal faults, Imai (1973) observed slickenside striations to conclude
340 that sinistral strike-slip components were dominant rather than dip-slip components on
341 the faults. This is consistent with the fact that the N-S trending faults hosted ore veins
342 preferentially at their jogs (Uehara, 1959). Their faulting is not explained by the reverse
343 faulting stress regime consistent with the folding but by the strike-slip stress regime

344 with an intermediate stress ratio and with the σ_3 -axis subparallel to the general trend of
345 folds in Tsushima. Kim et al. (2010) suggested the sinistral movements of N-S trending
346 offshore faults by NNW-SSE compression, but such a stress should have resulted in not
347 strike-slip but oblique normal faulting along the easterly dipping N-S trending faults in
348 the mine. The strike-slip faults displaced the 'bedding group' (Imai, 1973), suggesting
349 that the NW-SE compression responsible for the folding was followed by a strike-slip
350 faulting stress regime which backgrounded the final phase of ore mineralization (Fig.
351 16). Fabbri et al. (1996) inferred the sinistral movements along the Tsushima Fault
352 System and along N-S trending faults in Goto Islands (Fig. 1a) from 13 to 10 Ma. This
353 movement may have begun at ~15 Ma.

354 The detailed geological mapping by mining geologists concluded that the folded
355 Taishu Group was pierced by the granitic pluton to the southeast of the mine, suggesting
356 that the folding did not postdate the granite emplacement (Matsushashi et al., 1970). The
357 intrusion of quartz porphyry magmas into the group was no later than the granite
358 emplacement (Imai, 1973).

359 In conclusion, the Taishu Group was folded in the late Early to early Middle
360 Miocene before the granite emplacement to bring about NW-SE trending crustal
361 shortening (Fig. 2c). The folding involved the deformations of sills, dikes, and affected
362 ore veining.

363 4.3 Implications for regional tectonics

364 The weakness of the arguments about the folding in Tsushima based on onshore geology
365 comes from insufficient time control. Fortunately, since the turn of the century, some of
366 offshore geological data obtained by Chinese and Korean geologists became easily
367 accessible. They place constraints on the tectonic history of Japanese islands. Some
368 researchers thought that the folds in Tsushima are the onshore part of the Taiwan-Shinji
369 fold belt (e.g., Itoh & Nagasaki, 1996), which was formed mainly in the latest Miocene
370 (Cukur et al., 2011; Gungor et al., 2012; Kong et al., 2000; Lee et al., 2006, 2011;
371 Tanaka & Ogusa, 1981; Yoshioka et al., 2002). However, Korean geologists revealed
372 that the folding began at ~12 Ma (Fig. 16) (Kim et al., 2019; Lee et al., 2001, 2011;
373 Park et al., 2020; Yoon et al., 2002, 2003). It means that the folding in the belt was not
374 simultaneous with the main phase of the folding in Tsushima (Fig. 16). This conclusion
375 is based on the age of magmatism and ore veins in Tsushima, but a systematic work is
376 necessary for their precise dating. However, the uncertainty of the ages does not affect
377 this conclusion.

378 Japanese geologists suggested that the formation of the Taiwan-Shinji fold belt
379 began at ~15 Ma since Tai's (1973) work, but their arguments were based on indirect

380 evidence. That is, Middle Miocene isopach maps were used to argue the commencement
381 (Tai, 1973; Kano & Yoshida, 1985; Nomura, 1986), where a roughly horizontal
382 depositional surface was assumed to convert the lateral variation in stratal thickness to
383 the subsidence of a syncline more rapidly than that of a neighboring anticline. However,
384 this assumption is not always valid. On the other hand, the trends of parallel dike
385 swarms were thought to suggest the transition from extensional to compressional at ~15
386 Ma (Tsunakawa, 1986; Yamamoto, 1991), but it was recently shown (Haji and Yamaji,
387 submitted) that dikes in northern Hyogo prefecture where the tightest constraint for the
388 transition was presented by Kobayashi (1979a, b) did not evidence the transition.
389 Instead, Haji and Yamaji found extensional stress in the early Middle Miocene by means
390 of the stress inversion technique of Yamaji and Sato (2011). The thrusting of the Tobe
391 thrust—a part of the Median Tectonic Line in western Shikoku—at ~15 Ma was thought
392 to mark the beginning of the compression that formed the fold belt (e.g., Takeshita,
393 1993). However, the Tobe thrust is exceptional: There is no other map-scale,
394 contemporaneous thrust fault in SW Japan. Such an exceptional reverse fault can be
395 locally activated in extensional tectonics (Gabrielsen et al., 1997; Dooley et al., 2003).
396 A dike swarm near the Tobe thrust indicates extensional stress at 14–15 Ma (Yamaji &
397 Sato, 2011). However, the accretionary wedge off Shikoku was subjected to horizontal
398 compression at that time (Haji & Sato, 2020). Thus, SW Japan was subjected largely to
399 weak extension in the early Middle Miocene.

400 Folding in Tsushima was also argued in relation with the Japan Sea opening, which
401 occurred in the Early to early Middle Miocene. They attributed the folding of the Taishu
402 Group to the transpression (Fig. 2a, b) to accommodate the difference between the
403 rapidly opening Tsushima Basin and the East China Sea which the researchers thought
404 to be relatively stable at that time (Ishikawa & Tagami, 1991). Several researchers
405 accepted this hypothesis (Golozubov et al., 2017; Kim et al., 2010). However, this
406 hypothesis is inconsistent with the deformation styles in the Taishu Group found in this
407 study.

408 The folding was regarded by Sakai (1993) and Kim et al. (2010) to be
409 contemporaneous with the Japan Sea opening. Sakai assumed that the SW Japan arc and
410 the entire Kyushu belonged to a coherent block that rotated clockwise, and he assumed
411 the Euler pole of the drifting block to the east of Tsushima to explain the folding (Sakai,
412 1993, Fig. 11). This hypothesis is consistent with the orogen-perpendicular shortening
413 found in this study. The Philippine Sea plate migrated northwestward along the Ryukyu
414 trench in the Early Miocene (e.g., Hibbard & Karig, 1990). Kim et al. (2010) attributed
415 the positioning of the Euler pole to the arrival of the plate off Kyushu to explain the

416 folding in Tsushima.

417 The paleomagnetic rotation of SW Japan is expected to be simultaneous with the
418 folding if the folding is explained by the rotation. However, this explanation is unlikely
419 as follows. Paleomagnetic studies showed that the rotation occurred from ~18 to 16 Ma
420 (Hoshi, 2018; Hoshi et al., 2015; Tamaki et al., 2006). So, the rotation was possibly
421 accompanied by the early folding in Tsushima, but the folding simultaneous with the
422 formation of the ore veins cannot be explained by the rotation (Fig. 16). The Taishu
423 Group is thought to be a graben fill (Golozubov et al., 2017) or a result of extensional
424 tectonics (Kim et al., 2010), whereas the deposition of the group was terminated at ~16
425 Ma (Ninomiya et al., 2014). So, the youngest part of the group may have been
426 accumulated in the early folding stage. Changes in tectonic environment do not always
427 make unconformities as exemplified by the Neogene-Quaternary succession in the
428 Niigata basin, central Japan, where syn- and post-rift and inversion-stage strata are not
429 separated by unconformities (e.g., Takano, 2002).

430 Recent Chinese and Korean data indicate that the basins in the East China Sea and
431 Yellow Sea (Fig. 1a) were subjected to compression in the Early Miocene. It is
432 improbable that compression in those regions had direct causal relationship with the
433 Japan Sea opening (e.g., Cukur et al., 2011; Kong et al., 2000; Shin, 2015; Wang et al.,
434 2019; Yoon et al., 2010). Accordingly, we suggest that the folding in Tsushima was the
435 eastern most manifestation of the compressional tectonic regime around the Yellow Sea
436 and East China Sea. We suggest also that the triple trench junction of the Eurasia,
437 Pacific and Philippine Sea plate arrived off Kyushu at ~16 Ma. The plate model by Hall
438 et al. (1995, Fig. 10) seems consistent with this interpretation, though they do not show
439 the plate configuration at ~16 Ma. The buoyant subduction of the spreading Shikoku
440 basin in the Philippine Sea plate may have been responsible to the compressional stress
441 condition in and around Kyushu under which the Taishu Group was folded, while the
442 SW Japan arc was largely subjected to extensional stress.

443

444 5 SUMMARY

445

446 Most of mesoscale faults that we observed at outcrops had NW and SE vergence,
447 perpendicular to the axes of map-scale folds in in the Taishu Group. Bedding faults
448 involved by flexural-slip folding had the vergence as well. Those structures indicated
449 orogen-perpendicular shortening of the crust associated with the folding. Early to early
450 Middle Miocene dikes and sills were also involved in such deformations. Our
451 observations at the surface were consistent with the opinion given by the geologists of

452 Taishu Mine half a century ago based on their observations of ore veins in the mine.
453 That is, the strata were folded shortly before and simultaneously with older ore veins
454 that deposited at ca. 14.5–16.5 Ma. The compression at this timing was probably
455 brought about by the arrival of the Philippine Sea plate to initiate buoyant subduction
456 under Kyushu.

457

458 **ACKNOWLEDGEMENTS**

459

460 We are grateful to T. Nomoto for the guidance on the BSE and EDS analyses of ore
461 veins, H. Sakai and T. Tagami for discussions, T. Nakajo for referring us to
462 sedimentological articles, and anonymous reviewers and for constructive comments.
463 Special thanks are due to the Society of Resource Geology—the successor of the
464 Society of Mining Geologists of Japan—for the permission to reproduce the illustration
465 in Fig. 15. Constructive comments from anonymous reviewers improved the manuscript.
466 This work was supported partly by JSPS KAKENHI Grant Number 21740364.

467

468 **OCID**

469 *Atsushi Yamaji* 0000-0001-8074-543X

470 *Katsushi Sato* 0000-0001-9537-5064

471

472

473 **REFERENCES**

474

- 475 Chinzei, K. (1986). Opening of the Japan Sea and marine biogeography during the
476 Miocene. *Journal of Geomagnetism and Geoelectricity*, 38(5), 487–494.
- 477 Cukur, D., Horozal, S., Kim, D.C., & Han, H.C. (2011). Seismic stratigraphy and
478 structural analysis of the northern East China Sea Shelf Basin interpreted from
479 multi-channel seismic reflection data and cross-section restoration. *Marine and*
480 *Petroleum Geology*, 28(5), 1003–1022.
- 481 Dooley, T., McClay, K.R., & Pascoe, R. (2003). 3D analogue models of variable
482 displacement extensional faults: applications to the Revfallet Fault system, offshore
483 mid-Norway. In D.A. Nieuwland (Ed.), *New Insights into Structural Interpretation*
484 *and Modelling*, (pp. 151–167), Geological Society of London.
- 485 Elliott, D., & Johnson, M.R.W. (1980). Structural evolution in the northern part of the
486 Moine thrust belt. *Transactions of the Royal Society of Edinburgh*, 71(2), 69–96.
- 487 Fabbri, O., Charvet, J., & Fournier, M. (1996). Alternate senses of displacement along

488 the Tsushima fault system during the Neogene based on fracture analyses near the
489 western margin of the Japan Sea. *Tectonophysics*, 257(2-4), 275–295.

490 Fitches, W.R., Cave, R., Craig, J., & Maltman, A.J. (1986). Early veins as evidence of
491 detachment in the Lower Paleozoic rocks of the Welsh Basin. *Journal of Structural*
492 *Geology*, 8(6), 607–620.

493 Florez-Nino, J.M., Aydin, A., Mavko, G., Antonellini, M., & Ayaviri, A. (2005). Fault
494 and fracture systems in a fold and thrust belt: An example from Bolivia. *AAPG*
495 *Bulletin*, 8(4), 471–493.

496 Gabrielsen, R.H., Zalmstra, H., Sokoutis, D., Willingshofer, E., Faleide, J.I., & Braut,
497 H.L. (2019). The influence of mechanically weak layers in controlling fault
498 kinematics and graben configurations: Examples from analog experiments and the
499 Norwegian continental margin. *AAPG Bulletin*, 103(5), 1097–1110

500 Golozubov, V.V., Kasatkin, S.A., Yokoyama, K., Tsutsumi, Y., & Kiyokawa, S. (2017)
501 Miocene dislocations during the formation of the Sea of Japan basin: Case study of
502 Tsushia Island. *Geotectonics*, 51(4), 412–427.

503 Gungor, A., Lee, G.H., Kim, H.-J., Han, H.-C., Kang, M.-H., Kim, J., & Sunwoo, D.
504 2012. Structural characteristics of the northern Okinawa Trough and adjacent areas
505 from regional seismic reflection data: Geologic and tectonic implications.
506 *Tectonophysics*, 522–523, 198–207.

507 Haji, T., & Sato, K. (2020). Reverse-faulting regime of stress implied from middle
508 Miocene basaltic 6 intrusions around the Cape Muroto, Southwest Japan. *Journal of*
509 *the Geological Society of Japan*, 126(11), 621–630 (in Japanese with English
510 abstract).

511 Haji, T., & Yamaji, A. (submitted) Post-rift stress history of SW Japan inferred from
512 early to middle Miocene intrusions and meso-scale faults in the Tajima–Myokensan
513 area. *Island Arc*

514 Hall, R., Fuller, M., Ali, J.R., & Anderson, C.D., (1995). The Philippine Sea Plate:
515 Magnetism and reconstructions. In B. Taylor, & J. Natland (Eds.), *Active Margins*
516 *and Marginal Basins of the Western Pacific* (pp. 371–403) Washington, D.C.:
517 American Geophysical Union.

518 Hibbard, J.P., & Karig, D.E. (1990). Alternative plate model for the early Miocene
519 evolution of the southwest Japan margin. *Geology*, 18(2), 170–174.

520 Holdsworth, R.E., Tavarnelli, E., Clegg, P., Pinheiro, R.V. L., Jones, R.R., & McCaffrey,
521 K.J. W. 2002. Domainal deformation patterns and strain partitioning during
522 transpression: An example from the Southern Uplands terrane, Scotland. *Journal of*
523 *the Geological Society, London*, 159(4), 401–415.

- 524 Hoshi, H. (2018). Miocene clockwise rotation of SW Japan. *Journal of the Geological*
525 *Society of Japan*, 124(9), 675–691 (in Japanese with English abstract).
- 526 Hoshi, H., Kato, D., Ando, Y., & Nakashima, K. (2015). Timing of clockwise rotation of
527 Southwest Japan: Constraints from new middle Miocene paleomagnetic results.
528 *Earth, Planets and Space*, 67. <https://doi.org/10.1186/s40623-015-0266-3>.
- 529 Ibaraki, M. (1994). Ages and paleoenvironments of the Tertiary in northern Kyushu
530 inferred from planktonic foraminifers. *Chikyū*, 16, 150–153 (in Japanese).
- 531 Ikemi, H., Shimada, N., & Chiba, H. (2001). Thermochronology for the granitic pluton
532 related to lead-zinc mineralization in Tsushima, Japan. *Resource Geology*, 51(3),
533 229–238.
- 534 Imai, H. (1973). The geologic structure and mineralization at the Taishu Mine, Nagasaki
535 Prefecture, Japan. *Journal of the Mining and Metallurgical Institute of Japan*,
536 89(1026), 509–514 (in Japanese English abstract).
- 537 Inoue, E. (1982). Geological problems on Cretaceous and Tertiary rocks in and around
538 Tsushima-Korea straits. *U.N. ESCAP, CCOP Technical Bulletin*, 15, 85–121.
- 539 Ishikawa, N., & Tagami, T. (1991). Paleomagnetism and fission-track geochronology on
540 the Goto and Tsushima Islands in the Tsushima Strait area: Implications for the
541 opening of the Japan Sea. *Journal of Geomagnetism and Geoelectricity*, 43(3),
542 229–253.
- 543 Ishikawa, N., Torii, M., & Koga, K. (1989). Paleomagnetic study of the Tsushima
544 Islands, southern margin of the Japan Sea. *Journal of Geomagnetism and*
545 *Geoelectricity*, 41(9), 787–811.
- 546 Isomi, H., & Nagahama, H. (1965). Unconformity between the Taishu Group and the
547 Pliocene Ebishima Formation in the northernmost part of the Tsushima Islands,
548 west Japan: A contribution to the age problem of the Taishu Group. *Journal of the*
549 *Geological Society of Japan*, 71(832), 32–35 (in Japanese with English abstract).
- 550 Itoh, Y., & Nagasaki, Y. (1996). Crustal shortening of Southwest Japan in the Late
551 Miocene. *Island Arc*, 5(3), 337–353.
- 552 Jolivet, L., Huchon, P., Brun, J.P., Le Pichon, X., Chamot-Rooke, N., & Thomas, J.C.
553 (1991). Arc deformation and marginal basin opening: Japan Sea as a case study.
554 *Journal of Geophysical Research*, 96(B3), 4367–4384.
- 555 Jones, R.R., Holdsworth, R.E., Clegg, P., McCaffrey, K., & Tavarnelli, E. (2004).
556 Inclined transpression. *Journal of Structural Geology*, 26(8), 1531–1548.
- 557 Kano, K., & Yoshida, S. (1985). *Geology of the Sakaiminato District*. Quadrangle Series,
558 1:50,000. Geological Survey of Japan, AIST (in Japanese with English abstract).
- 559 Karakida, Y. (1987). K-Ar ages of the igneous rocks in Tsushima Shimojima, Nagasaki

- 560 Prefecture. *Journal of Nikkan Tunnel Study Group*, 7, 32–42 (in Japanese).
- 561 Kim, H.G., Song, C.W., Kim, J.S., Son, M., & Kim, I.S. (2008). Tertiary Geological
562 Structures and Deformation History of the Southern Tsushima Island, Japan.
563 *Journal of the Geological Society of Korea*, 44, 175–198 (in Korean).
- 564 Kim, H., Song, C.W., Son, M., Koo, H., & Bautista, F.E. (2010). Crustal deformation
565 history of the Tsushima Island and its vicinity, Japan, during the Cenozoic Tertiary.
566 *44th US Rock Mechanics Symposium and 5th US/Canada Rock Mechanics*
567 *Symposium*, ARMA10-371.
- 568 Kim, K.-J., Yoo, D.-G., Kang, N.-K., & Yi, B.-Y. (2019). Tectonostratigraphic
569 framework and depositional history of the deepwater Ulleung Basin, East Sea/Sea
570 of Japan. *Basin Research*, 32(4), 613–635.
- 571 Kimura, S., Shikazono, N. Kashiwagi, H., & Nohara, M. (2004). Middle Miocene–early
572 Pliocene paleo-oceanic environment of Japan Sea deduced from geochemical
573 features of sedimentary rocks. *Sedimentary Geology*, 164(1-2), 105–129.
- 574 Kitamura, A., & Kimoto, K. (2006). History of the inflow of the warm Tsushima
575 Current into the Sea of Japan between 3.5 and 0.8 Ma. *Palaeogeography,*
576 *Palaeoclimatology, Palaeoecology*, 236(3-4), 355–356.
- 577 Kitamura, N. (1962). Preliminary report on systematic jointing in the Taishu Group
578 developed in Mitsushima-cho, Tsushima Islands, Japan. Science Reports of Tohoku
579 University, 2nd Ser., Geology, 5, 303–319.
- 580 Kiyosu, Y. (1977). Sulfur isotope ratios of ores and chemical environment of ore
581 deposition in the Taishu Pb-Zn sulfide deposits, Japan. *Chemical Geology*, 11(2),
582 91–99.
- 583 Kobayashi, Y. (1979a). Late Neogene dike swarms and regional tectonic stress field in
584 the inner belt of Southwest Japan. *Bulletin of the Volcanological Society of Japan,*
585 *2nd Ser.*, 24(3), 153–168 (in Japanese with English abstract).
- 586 Kobayashi, Y. (1979b). Early and Middle Miocene dike swarms and regional tectonic
587 stress field in the Southwest Japan. *Bulletin of the Volcanological Society of Japan,*
588 *2nd Ser.*, 24(4), 203–212 (in Japanese with English abstract).
- 589 Koga, H., Taira, A., Ashi, J., Kuramoto, S., & Fujioka, K. (1988). A big collapsing in
590 delta front: an example of the Taishu Group, Tsushima. *Earth Monthly (Gekkan*
591 *Chikyu)*, 10, 516–522 (in Japanese).
- 592 Kong, F., Lawver, L.A., & Lee, T.-Y. (2000). Evolution of the southern Taiwan-Shinzi
593 folded zone and opening of the southern Okinawa trough. *Journal of Asian Earth*
594 *Sciences*, 18(3), 325–341.
- 595 Lee, G.H., Kim, H.J., Han, S.J., & Kim, D.C. (2001). Seismic stratigraphy of the deep

- 596 Ulleung Basin in the East Sea (Japan Sea) back-arc basin. *Marine and Petroleum*
597 *Geology*, 18(5), 615–634.
- 598 Lee, G. H., Yoon, Y. H., Nam, B. H., Lim, H. H., Kim, Y. S., Kim, H. J., & Lee, K. S.
599 (2011). Structural evolution of the southwestern margin of the Ulleung Basin, East
600 Sea (Japan Sea) and tectonic implications. *Tectonophysics*, 502(3-4), 293–307.
- 601 Lee, G.H., Kim, B., Shin, K.S., & Sunwoo D. (2006). Geologic evolution and aspects of
602 the petroleum geology of the northern East China Sea shelf basin. *AAPG Bulletin*,
603 90(2), 237–260.
- 604 Lee, S.A., & Son, B.-K. (2016). Petroleum system modeling of the Sora basin, offshore
605 southern Korea. *Journal of the Geological Society of Korea*, 52(3), 333–353 (in
606 Korean with English abstract).
- 607 Matsushashi, S. (1967). Structural control and prospecting of the bedding plane veins in
608 the Taishu Mine. *Mining Geology*, 17(82-83), 151–161 (in Japanese with English
609 abstract).
- 610 Matsushashi, S. (1968). Analysis of structural control and results of prospecting for
611 bedding-plane veins in the Taishu Mine. *Mining Geology*, 18(90), 161–172 (in
612 Japanese with English abstract).
- 613 Matsushashi, S., Kiri, K., Nakashima, Y., Fukumoto, K., Nemoto, T., & Kuronuma, C.
614 (1970). Geology of the Taishu Mine area in Shimo-shima, Tsushima Islands.
615 *Memoirs of the National Science Museum*, 3, 1–8 (in Japanese with English
616 abstract).
- 617 Matsumoto, Y., & Takahashi, K. (1987). Igneous activities in the Tsushima islands,
618 Nagasaki Prefecture, Japan. *Association for Geological Collaboration in Japan*
619 *Monograph*, 33, 1–20 (in Japanese with English abstract).
- 620 Matsumoto, T. (1969). Geology of Tsushima and relevant problems. *Memoirs of the*
621 *National Science Museum, Tokyo*, 2, 5–14 (in Japanese with English abstract).
- 622 McClay, K.R. (1992). Glossary of thrust tectonics terms. In K.R. McClay (Ed.) *Thrust*
623 *Tectonics* (pp. 419–433), London, UK: Chapman & Hall.
- 624 Millien-Parra, V., & Jaeger, J.J. (1999). Island biogeography of the Japanese terrestrial
625 mammal assemblages: An example of a relict fauna. *Journal of Biogeography*,
626 26(5), 959–972.
- 627 Minami, A. (1979). Distribution and characteristics of the sedimentary basin offshore
628 San-in to Tsushima Island. *Journal of Japanese Association of Petroleum*
629 *Technologists*, 44(5), 321–328 (in Japanese with English abstract).
- 630 Miyata, Y. (2010). Tertiary Systems of Tsushima, Goto and Iki. In H. Sano *et al.* (Eds.)
631 *Regional Geology of Japan*, vol. 8, Kyushu (pp. 85–87), Tokyo: Asakura Publishing

- 632 Co.
- 633 Nakajo, T., & Funakawa, T. (1996). Eocene radiolarians from the Lower Formation of
634 the Taishu Group, Tsushima Islands, Nagasaki Prefecture, Japan. *Journal of the*
635 *Geological Society of Japan*, 102(8), 751–754 (in Japanese).
- 636 Nakajo, T., & Maejima, W. (1998). Morpho-dynamic development and facies
637 organization of the Tertiary delta system in the Taishu Group, Tsushima Islands,
638 southwestern Japan. *Journal of the Geological Society of Japan*, 104(11), 749–763.
- 639 Nakajo, T., Yamaguchi, Y., Komatsubara, J., & Ohtake, S. (2006). Sedimentation and
640 tectonics of the Tertiary delta to basin successions in the Tsushima Islands, off
641 northwestern Kyushu, Japan. *Field Excursion Guidebook, 17th International*
642 *Sedimentological Congress, Fukuoka, Japan*, FE-B11, 1–12.
- 643 Ninomiya, T., Taniguchi, S., Shimoyama, S., Miyata, Y., Dunkley, D.J., Matsuda, H.,
644 Yamanaka, T., Aoki, T., Nishida, T., & Ichihara, T. (2009). Formative age and
645 sedimentary environment of the Taishu Group, Nagasaki Prefecture, Southwest
646 Japan. *Abstracts, the Annual Meeting of the Geological Society of Japan* 67 (in
647 Japanese).
- 648 Ninomiya, T., Taniguchi, S., Shimoyama, S., Miyata, Y., Dunkley, D.J., Matsuda, H.,
649 Yamanaka, T., Aoki, T., Nishida, T., & Ichihara, T. (2010). Sedimentary enviroment
650 of the Neogene Taishu Group, Nagasaki Prefecture, southwest Japan. *Abstracts, the*
651 *Annual Meeting of the Geological Society of Japan*, 131 (in Japanese).
- 652 Ninomiya, T., Shimoyama, S., Watanabe, K., Horie, K., Dunkley, D.J., & Shiraishi, K.
653 (2014). Age of the Taishu Group, southwestern Japan, and implications for the
654 origin and evolution of the Japan Sea. *Island Arc*, 23(3), 206–220.
- 655 Ninomiya, T., Shimoyama, S., Taniguchi, S., Takahashi, T., Danhara, T. & Iwano, H.
656 (2019). Age of the Tsushima Lapilli Tuff and implication for Japan Sea opening.
657 *Abstracts, the Annual Meeting of the Geological Society of Japan*, 14 (in Japanese).
- 658 Ninomiya, T., Shimoyama, S., Miyata, Y., Yamanaka, T., Shimazu, T., Taniguchi, S.,
659 Aoki, T., Nishida, T. & Takahashi, T. (2020). Origin and water depth of a newly
660 identified seep carbonate and paleoecology of *Bathymodiolus* in the Miocene
661 Taishu Group, southwestern Japan. *Palaeogeography, Palaeoclimatology,*
662 *Palaeoecology*, 546, 109655.
- 663 Nomura, R. (1986). Geology of the central part in the Shimane Peninsula: Part 1
664 Miocene stratigraphy. *Journal of the Geological Society of Japan*, 92(6), 405–420
665 (in Japanese with English abstract).
- 666 Oho, Y., Yamaguchi, Y., & Hirayama, Y. (2007). Incipient slaty cleavage in the Taishu
667 Group of north Tsushima Islands, southwest Japan. *Journal of the Geological*

- 668 *Society of Japan*, 113(4), 146–157 (in Japanese with English abstract).
- 669 Okada, H. (1969). A preliminary study of the geological section across the northern area
670 of the Tsushima Islands, Kyushu. *Memoirs of the National Science Museum, Tokyo*,
671 2, 19–28 (in Japanese with English abstract).
- 672 Okada, H., & Fujiyama, I. (1970). Sedimentary cycles and sedimentation of the Taishu
673 Group in the Shiohama area, central Tsushima, Kyushu. *Memoirs of the National*
674 *Science Museum*, 3, 9–17 (in Japanese with English abstract).
- 675 Park, Y., Yoo, D., Kang, N., Yi, B., & Kim B. (2020). Tectonic control on
676 mass-transport deposit and canyon-fed fan system in the Ulleun Basin, East Sea
677 (Sea of Japan). *Basin Research*, 32(4), 613–635.
- 678 Petit, J.-P. (1987). Criteria for the sense of movement on fault surfaces in brittle rocks.
679 *Journal of Structural Geology*, 9(5-6), 597–608.
- 680 Ramsay, J. (1967). *Folding and Fracturing of Rocks*. New York: McGraw-Hill.
- 681 Sakai, H. (1993). Tectonics and sedimentation of the Tertiary sedimentary basins in the
682 northern Kyushu. *Geological Society of Japan Memoir*, 42, 183–201 (in Japanese
683 with English abstract).
- 684 Sakai, H., & Nishi, H. (1990). Geologic ages of the Taishu Group and the Katsumoto
685 Formation in the Tsushima and Iki Islands, off Kyushu on the basis of planktonic
686 foraminifers. *Journal of Geological Society of Japan*, 96(5), 389–392.
- 687 Sakai, H., & Yuasa, T. (1998). K-Ar ages of the Mogi and Ugetsuiwa subaqueous
688 pyroclastic flow deposits in the Taishu Group, Tsushima Islands. *Memoir of*
689 *National Science Museum, Tokyo*, 31, 23–28 (in Japanese with English abstract).
- 690 Sato, K. (2006). Incorporation of incomplete fault-slip data into stress tensor inversion.
691 *Tectonophysics*, 421(3-4), 319–330.
- 692 Scheidegger, A.E. (1965). On the statistics of the orientation of bedding planes, grain
693 axes, and similar sedimentological data. *USGS Professional Paper*, 525-C,
694 164–167.
- 695 Shimada, N. (1977). Lead-zinc ore deposits of the Tsushima Islands, Nagasaki
696 Prefecture, with special reference to Shigekuma-type mineralization. *Memoirs of*
697 *the Faculty of Science, Kyushu University*. D23, 417–480 (in Japanese with English
698 abstract).
- 699 Shin, K.-C., Kurosawa, M., Anma, R. & Nakano, T. (2009). Genesis and
700 mixing/mingling of mafic and felsic magmas of back-arc granite: Miocene
701 Tsushima Pluton, Southwest Japan. *Resource Geology*, 59(1), 25–50.
- 702 Shin, Y.-J. (2015) Geological structures and controls on half-graben inversion in the
703 western Gunsan Basin, Yellow Sea. *Marine and Petroleum Geology*, 68, 480–491.

- 704 Silver, A.G. (1988). Strike-slip faults. *GSA Bulletin*, 100(11), 1666–1703.
- 705 Society of Mining Geologists of Japan (1968). Pictorial: Taishu Mine, Toho Zinc
706 Company. *Mining Geology*, 18(92), Plates 1–2 (in Japanese).
- 707 Suppe, J. (1983). Geometry and kinematics of fault-bending folding. *American Journal*
708 *of Science*, 283(7), 684–721.
- 709 Tai, Y. (1973). On the “Shinji Folded Zone.” *Memoir of Geological Society of Japan*, 9,
710 137–146 (in Japanese with English abstract).
- 711 Takahashi, K., & Hayashi, M. (1985). Fission-track ages of igneous rocks from
712 Tsushima Islands (I). *Bulletin of Faculty of Liberal Arts, Nagasaki University.*
713 *Natural science*, 25, 9–19.
- 714 Takahashi, K., & Hayashi, M. (1987). Fission-track ages of igneous rocks from
715 Tsushima Islands (II). *Bulletin of Faculty of Liberal Arts, Nagasaki University.*
716 *Natural Science*, 27, 19–31.
- 717 Takeshita, T. (1993). Deformation of the forearc region and along the Median Tectonic
718 Line in Southwest Japan during the opening of the Japan Sea: A preliminary report.
719 *Memoirs of the Geological Society of Japan*, 42, 215–244 (in Japanese with English
720 abstract).
- 721 Takano, O. (2002) Changes in depositional systems and sequences in response to basin
722 evolution in a rifted and inverted basin: an example from the Neogene
723 Niigata-Shin’etsu basin, Northern Fossa Magna, central Japan. *Sedimentary*
724 *Geology*, 152, 79–97.
- 725 Tamaki, M., Itoh, Y., & Watanabe, M. (2006). Paleomagnetism of the Lower to Middle
726 Miocene Series in the Yatsuo area, eastern part of southwest Japan: Clockwise
727 rotation and marine transgression during a short period. *Bulletin of the Geological*
728 *Survey of Japan*, 57, 73–88 (in Japanese with English abstract).
- 729 Tanaka, T., & Ogusa, K. (1981). Structural movement since middle Miocene in the
730 offshore San-in sedimentary basin, the Sea of Japan. *Journal of the Geological*
731 *Society of Japan*, 87(11), 725–736.
- 732 Tanner, P.W.G. (1989). The flexural-slip mechanism. *Journal of Structural Geology*,
733 11(6), 635–655.
- 734 Tavarnelli, E., Holdsworth, R.E., Clegg, P., Jones, R.R., & McCaffrey, K.J.W. (2004).
735 The anatomy and evolution of a transpressional imbricate zone, Southern Uplands,
736 Scotland. *Journal of Structural Geology*, 26(8), 1341–1360.
- 737 Tokuyama, H., Honza, E., Kimura, M., Kuramoto, S., Ashi, J., Okamura, Y., Arato, H.,
738 Itoh, Y., Soh, W., Hino, R., Nohara, T., Abe, H., Sakai, S., & Mukaiyama, K. (2001).
739 Tectonic development in the regions around Japan since latest Miocene. *Journal of*

740 *the Japan Society for Marine Surveys and Technology*, 13(1), 27–53 (in Japanese
741 with English abstract).

742 Tomita, S., Yamashita, A., Ishibashi, K., Miki, T., Takahashi, R., Shuto, T., Urata, H.,
743 Hashimoto, I., Honza, E., & Igarashi, C. (1975). Submarine geology west of the
744 Tsushima Islands. *Science Report, Department of Geology, Kyushu University*, 12,
745 77–90.

746 Tonai, S., Sato, K., & Ashi, J. (2011). Incremental fold test for paleostress analysis using
747 the Hough transform inverse method. *Journal of Structural Geology*, 33(7),
748 1158–1168.

749 Tsunakawa, H. (1986). Neocene stress field of the Japanese arcs and its relation to
750 igneous activity. *Tectonophysics*, 124(1-2), 1–22.

751 Twiss, R.J., & Gefell, M.J. (1990). Curved slickenfibers—a new brittle shear sense
752 indicator with application to a sheared serpentinite. *Journal of Structural Geology*,
753 12(4), 471–481.

754 Twiss, R.J., & Moores, E.M. (2007). *Structural Geology, 2nd Edition*. New York: W.H.
755 Freeman.

756 Uehara, Y. (1959). On the ore deposit and prospecting in the Taisyu Mine, Nagasaki
757 Prefecture. *Mining Geology*, 9, 265–275 (in Japanese with English abstract).

758 Uehara, Y., & Matsuhashi, S. (1961). Structural localization of ore shoot at the Taishu
759 Mine, Nagasaki Prefecture, Japan. *Mining Geology*, 11(45-46), 99–103 (in Japanese
760 with English abstract).

761 Wang, B., Doust, H., & Liu, J. (2019). Geology and petroleum systems of the East
762 China Sea Basin. *Energies*, 12(21), 4088, doi:10.3390/en12214088.

763 Watanabe, M., & Ikeda, Y. (1989). Sasuna, Mine, Nii and Izuhara. In The Research
764 Group for Active Tectonics in Kyushu (Ed.) *Active Tectonics in Kyushu* (pp. 72–79),
765 Tokyo: Tokyo University Press.

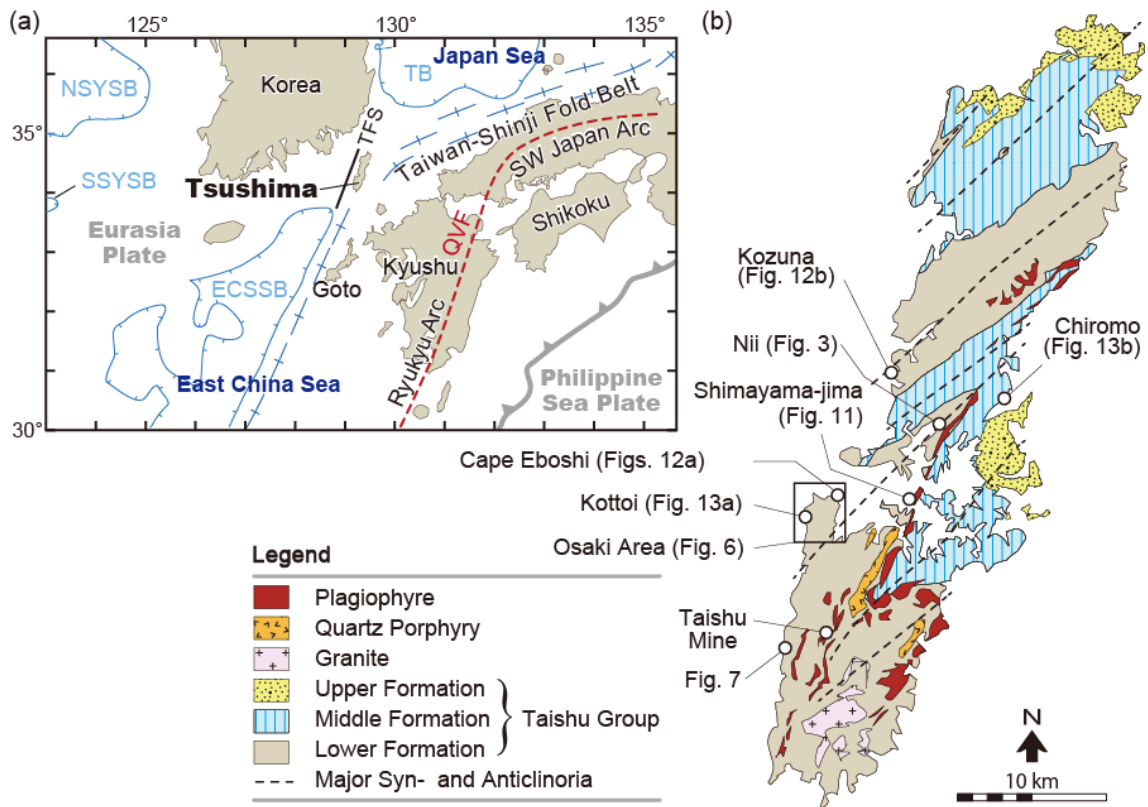
766 Wilcox, R.E., Harding, T.P., & Seely, R.D. (1973). Basic wrench tectonics. *AAPG*
767 *Bulletin*, 57(1), 74–96.

768 Yamaji, A., & Sato, K. (2011). Clustering of fracture orientations using a mixed
769 Bingham distribution and its application to paleostress analysis from dike or vein
770 orientations. *Journal of Structural Geology*, 33(7), 1148–1157.

771 Yamaji, A., Tomita, S. & Otsubo, M. (2005). Bedding tilt test for paleostress analysis.
772 *Journal of Structural Geology*, 27(1), 161–170.

773 Yamamoto, T. (1991). Late Cenozoic dike swarms and tectonic stress field in Japan.
774 *Bulletin of Geological Survey of Japan*, 42(3), 131–148 (in Japanese with English
775 abstract).

- 776 Yoon, S., Chough, S., & Park, S. (2003). Sequence model and its application to a
777 Miocene shelf-slope system in the tectonically active Ulleung Basin margin, East
778 Sea (Sea of Japan). *Marine and Petroleum Geology*, 20(10), 1089–1103.
- 779 Yoon, S.H., Park, S.J., & Chough, S.K. (2002). Evolution of sedimentary basin in the
780 southwestern Ulleung Basin margin: Sequence stratigraphy and geologic structures.
781 *Geosciences Journal*, 6(2), 149–159.
- 782 Yoon, Y., Lee, G.H., Han, S., Yoo, D.G., Han, H.C., Choi, K., & Lee, K. (2010).
783 Cross-section restoration and one-dimensional basin modeling of the Central
784 Subbasin in the southern Kunsan Basin, Yellow Sea. *Marine and Petroleum*
785 *Geology*, 27(7), 1325–1339.
- 786



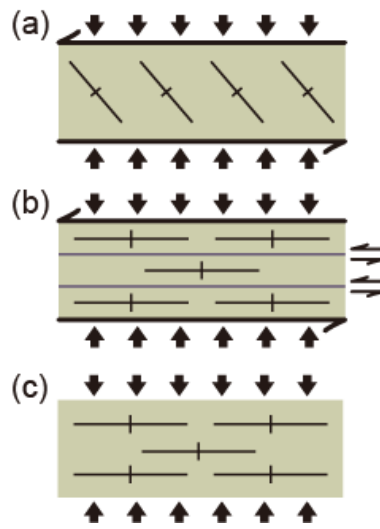
787

788

789 **FIGURE 1** (a) Tectonic map around Tsushima. Dashed line indicates the Quaternary
 790 volcanic front. The outline of the East China Sea Basin is after Lee et al. (2006), and
 791 those of the Northern and Southern South Yellow Sea Basins (NSYSB and SSYSB) are
 792 after Yoon et al. (2010). QVF, Quaternary volcanic front; TB, Tsushima Basin; TFS,
 793 Tsushima Fault System. (b) Geologic map of Tsushima Islands simplified from the
 794 compile map of Miyata (2010).

795

796



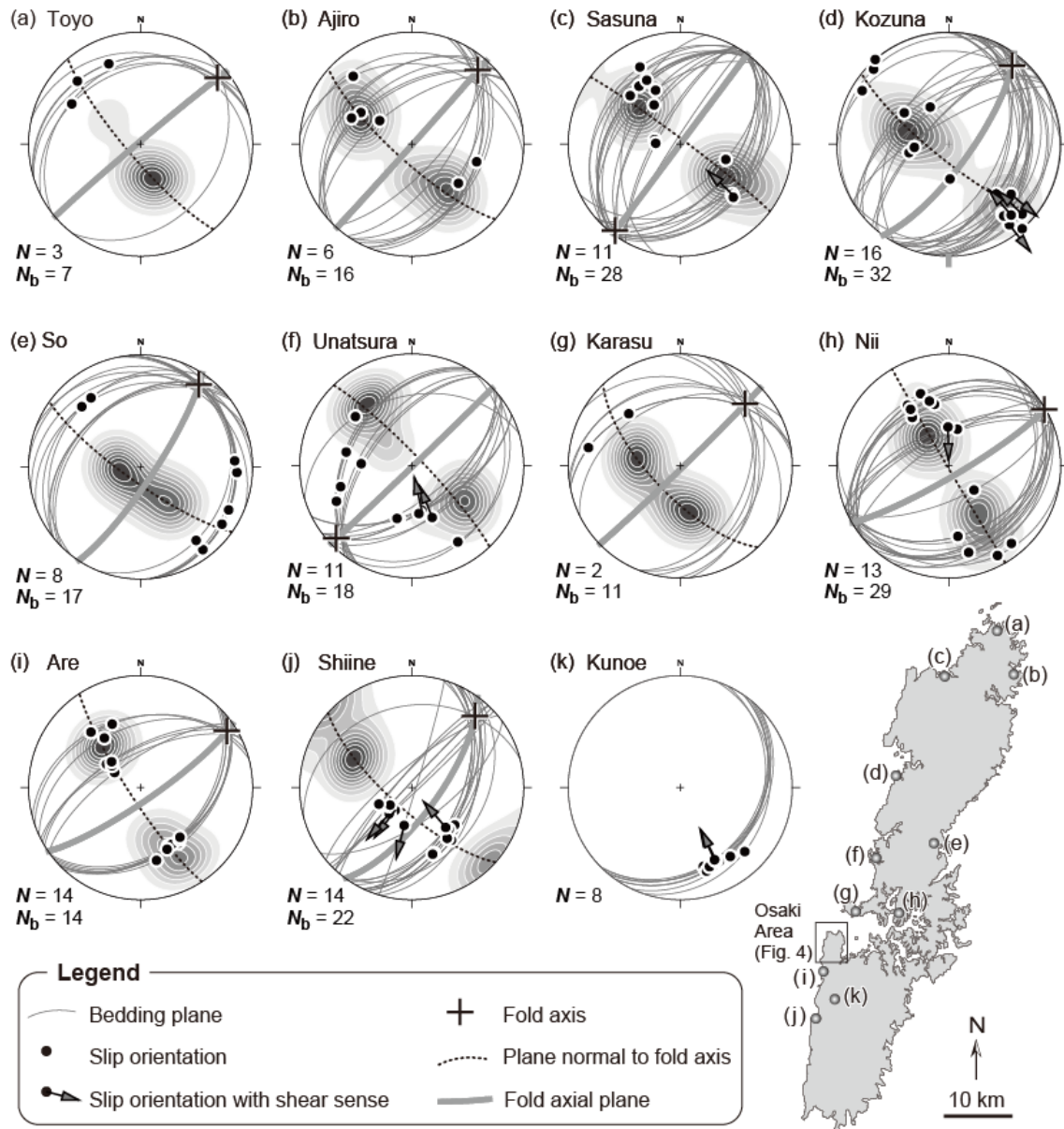
797
 798
 799
 800
 801
 802
 803
 804
 805
 806

FIGURE 2 Schematic plan views of folds in orogens with (a, b) and without (c) significant orogen-parallel shear. Bold arrows represent the shortening of the orogenic belts, and crosses indicate folds. (a) Echelon folds in a transpressional zone, one or both sides of which are bounded by strike-slip fault(s). (b) Folds and strike-slip faults accommodating the deformations perpendicular to and parallel to the orogen, respectively. (c) Folds with similar trends accommodating the shortening perpendicular to the orogen.



807
 808
 809
 810

FIGURE 3 An outcrop at near the port of Nii (Fig. 1b) showing mudstone with bedding and slaty cleavage.



811

812

813 **FIGURE 4** Lower-hemisphere, equal-area projections showing the attitudes of

814 structural elements in neighboring fold limbs. Thin lines and arrows attached to the lines

815 in the diagrams indicate the attitudes of bedding-parallel faults and the slip directions of

816 hanging-wall blocks, respectively. Great circles without arrows represent the

817 bedding-parallel faults whose senses of faulting were not determined. Contours in each

818 diagram show the number density of bedding poles. Axial planes were determined by

819 eyes as the central plane of the two clusters made by the poles in neighboring limbs.

820

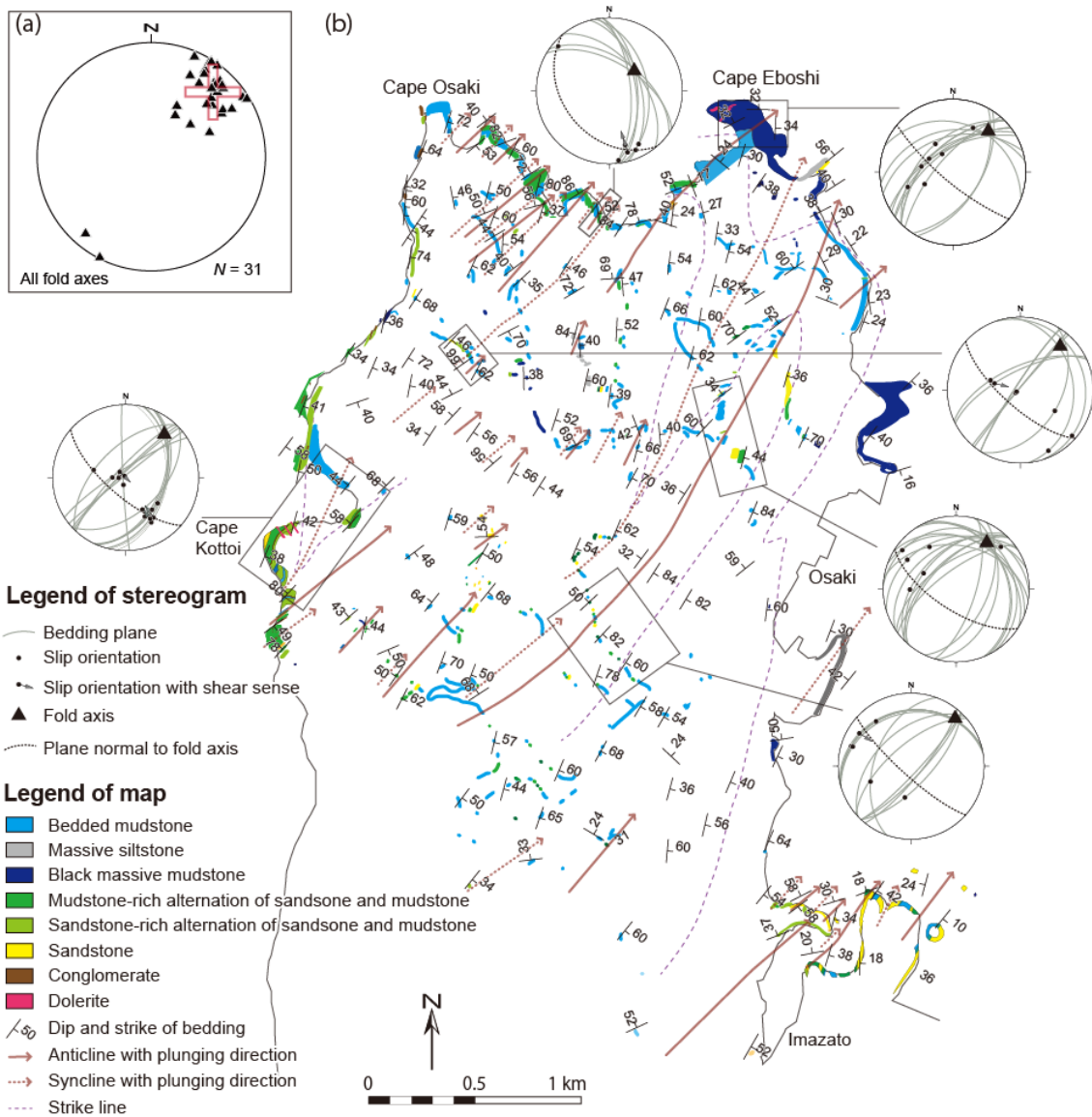


821

822

823 **FIGURE 5** The hinge zone of an open fold in the hinge zone of the map-scale anticline
824 at Cape Eboshizaki (Figs. 1b, 6b). Faulting along bedding planes (white lines) is
825 evidenced by quartz veins truncated at the planes. These brittle deformations evidence
826 the tectonic origin of the open fold. Variation of their apparent displacements along one
827 of the faults is due to the variation of vein orientations.

828



829

830

831 **FIGURE 6** Field map of the Osaki area. Location is shown in Fig. 1b. Stereograms
 832 show the geometry of folds with bedding-parallel faults. The inset shows all fold axes
 833 around Osaki area. The stereograms use lower-hemisphere and equal-area projection.

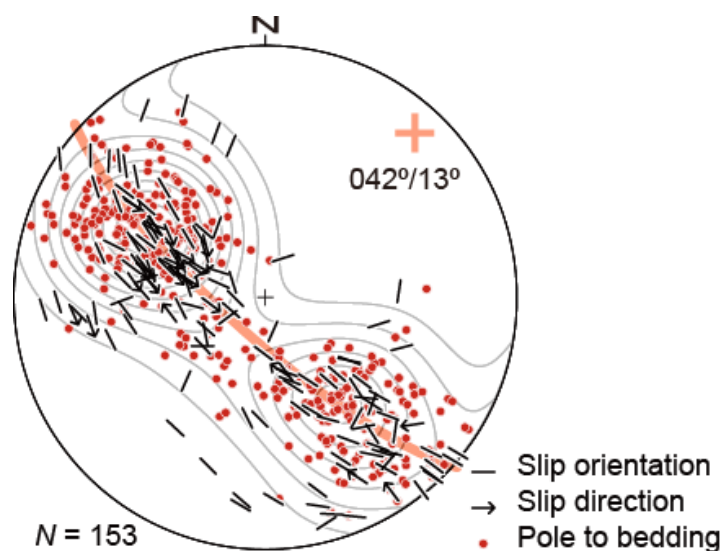
834



835

836 **FIGURE 7** (a) Overturned strata (shale and platy fine sandstone) to the south of Mt.
 837 Tohminodan (Fig. 1b). (b) Bedding parallel faults (arrows) indicated by quartz veins
 838 offset along bedding planes. The variation of their apparent displacements along a fault
 839 is due to the variation of vein attitudes.

840

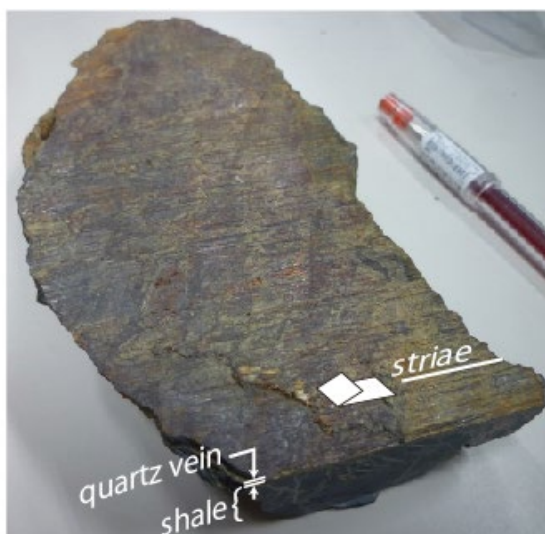


841

842

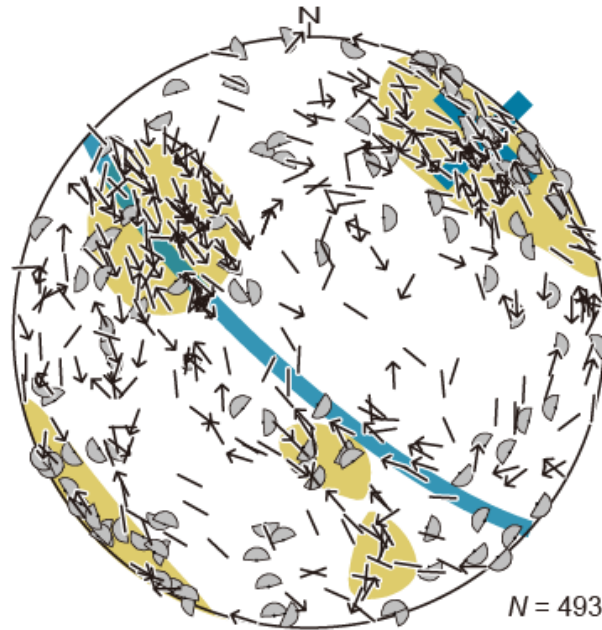
843 **FIGURE 8** Lower-hemisphere, equal-area projection of slip directions (arrows) and slip
 844 orientations (bars) of bedding-parallel faults in Tsushima. A total of 153 bars and arrows

845 are plotted. The positions of the symbols in the projection indicate the poles to the fault
846 plane. Arrows indicate the slip direction of footwall blocks. Poles to bedding planes are
847 denoted by dots, the density of which is shown by contours. Blue cross indicates the
848 representative orientation of fold axes that was obtained as the eigenvector
849 corresponding to the minimum eigenvalue of the orientation distribution tensor made
850 from the poles. Blue line indicates the great-circle perpendicular to the representative
851 orientation.
852



853
854
855
856
857

FIGURE 9 Slickenside striations on a bedding-parallel fault, the surface of which is coated by the ore vein including Zn- and Fe-rich minerals. Bold arrow depicts the sense of faulting. This sample was obtained near the Kunoe pit, Taishu Mine (Fig. 1b).



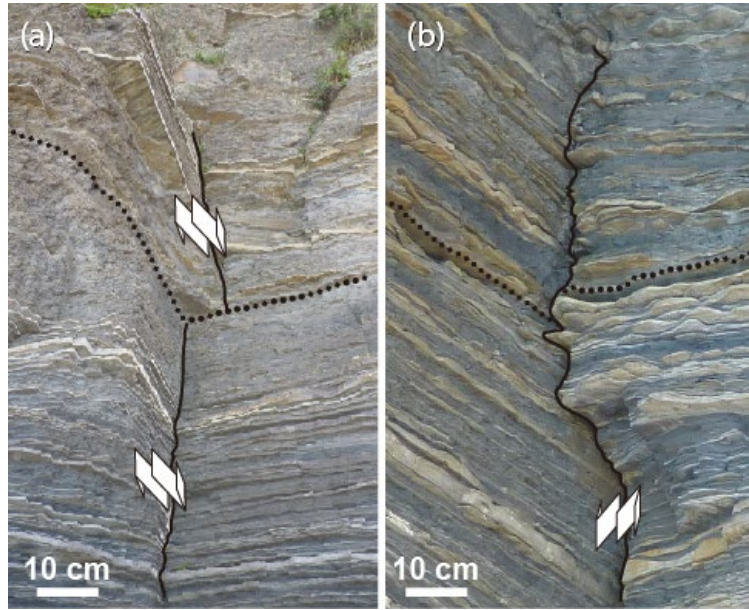
↗ Full data / Line only data / Sense only data

858

859

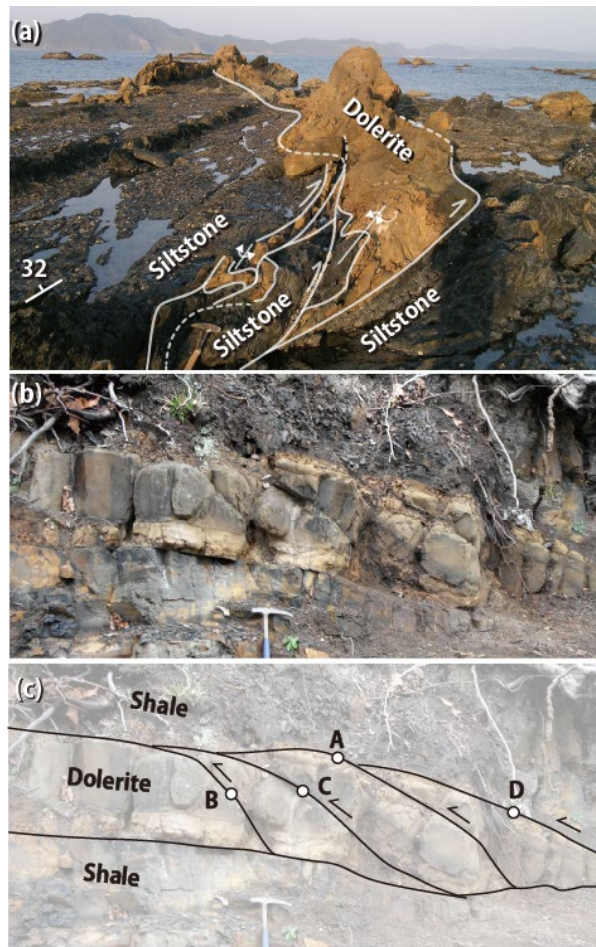
860 **FIGURE 10** Fault-slip data obtained from mesoscale faults excluding bedding-parallel
 861 faults in the Taishu Group. The data are denoted by the tangent-lineation diagram (Twiss
 862 & Gefell, 1990) improved by Sato (2006) to plot data with deficiency.
 863 Lower-hemisphere, equal-area projection. An arrow represents a datum without
 864 deficiency: The position and direction of the arrow indicate the pole to a fault plane and
 865 the slip direction of the footwall, respectively. Line only and sense only data are
 866 incomplete fault-slip data. That is, the former type of data was obtained from such faults
 867 that their senses were not determined but striations were observed, and the latter type of
 868 data were obtained from such faults that striations were not observed by their senses
 869 were determined using the offset of reference planes such as bedding. In this case, the
 870 slip direction of a footwall block was constrained with the uncertainty of 180°.
 871 Fan-shaped symbols are plotted for this reason. Yellowish areas indicate clusters. Bold
 872 blue cross and thick blue line show the mean orientation of fold axes and the
 873 great-circle perpendicular to the orientation.

874



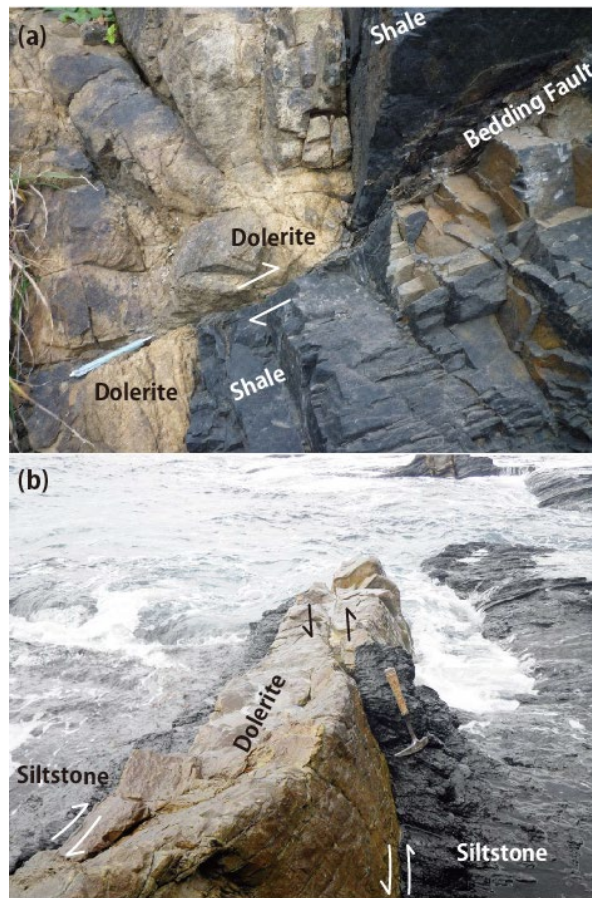
875
876
877
878
879

FIGURE 11 Cross-cutting relationship of bedding-parallel faults (dotted line) and NW-trending, mesoscale, strike-slip faults (solid line) at Shimayama-jima (Fig. 1b).



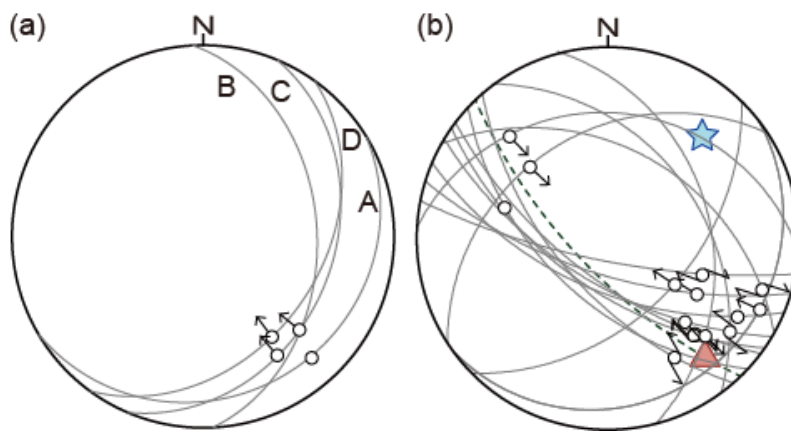
880

881 **FIGURE 12** Duplexes involving dolerite sills. (a) A duplex made of originally a single
 882 sill with changing thickness in northward dipping strata at the cape Eboshi. (b, c) An
 883 NW-vergent, hinterland-dipping duplex near Kozuna (Fig. 1b). The locations are shown
 884 in Fig. 1b. Fault-slip data obtained from the points A, B, C and D are shown in Fig. 13a.
 885



886
 887
 888
 889
 890
 891
 892

FIGURE 13 (a) A dolerite dike at Kottoi cut by a bedding-parallel fault, the hanging-wall of which moved northwestward. (b) Strike-slip duplex involving a NW-SE trending dolerite dike at Chiromo. The movements of the horses were subparallel to the trend of the dike (Fig. 14b). See Fig. 1b for the localities.



893
 894
 895

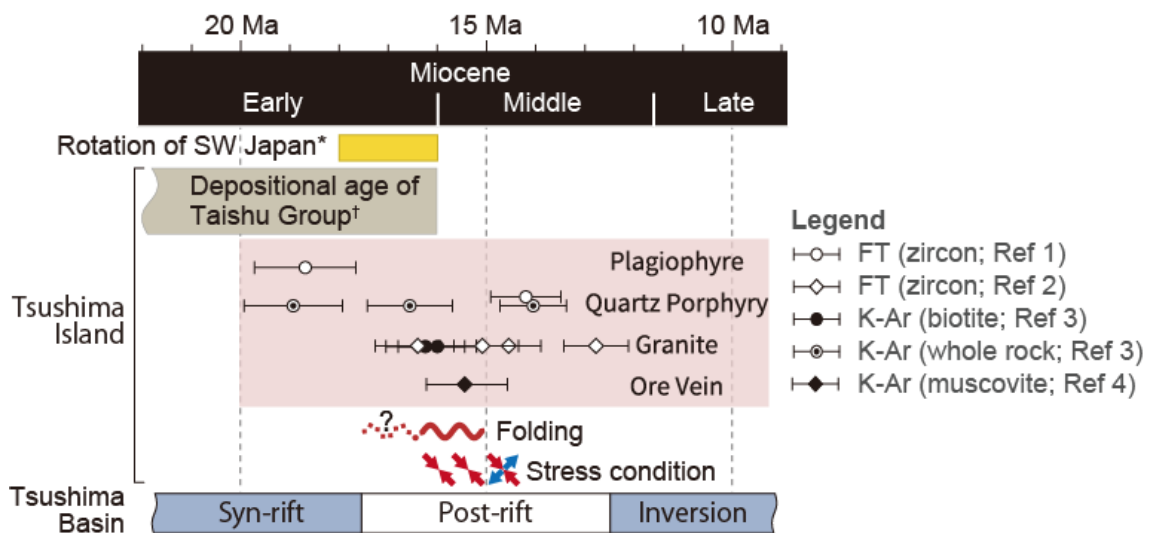
FIGURE 14 (a) Lower-hemisphere, equal-angle projection showing the fault-slip data

896 from the planes, A through D, between the horses of the duplex affecting the dolerite sill
 897 in Fig. 12c. The sense of movement on the plane A was not determined. (b) The data
 898 from the strike-slip duplex in Fig. 13b, and the σ_1 - and σ_3 -axes determined from them
 899 (triangle and star). Dotted line denotes the attitude of the dolerite dike.
 900



901

902 **FIGURE 15** A sketch showing ore veins formed preferentially at the dilational jogs of
 903 folds in the Taishu mine (The Society of Mining Geologists of Japan, 1968).
 904



905

906

907 **FIGURE 16** Radiometric ages of intrusive rocks in Tsushima with their $\pm 1\sigma$ error bars.
 908 Deposition of the Taishu Group ceased at ~20 or possibly at ~16 Ma. References:
 909 *Tamaki et al. (2006), Hoshi et al. (2015), Hoshi (2018); †Nakajo and Funakawa (1996),
 910 Ninomiya et al. (2014, 2019), Sakai and Nishi (1990), Sakai and Yuasa (1998); 1,
 911 Takahashi and Hayashi (1985); 2, Ishikawa and Tagami (1991); 3, Karakida (1987); 4,

912 Ikemi *et al.* (2001). Tectonic history in the Tsushima Basin after Kim *et al.* (2019).
913